Importance of Quantum Effects for C−H Bond Activation Reactions

Joaquín Espinosa-García,† José C. Corchado, and Donald G. Truhlar*

Contribution from the Department of Chemistry and Supercomputer Institute, University of Minnesota, Minneapolis, Minnesota 55455-0431

Received July 3, 1997[⊗]

Abstract: We calculate the reaction rate constant of the rearrangement of *trans*-$Rh(PH_3)_2Cl(\eta^2\text{-}CH_4)$ to $Rh(PH_3)_2ClH(CH_3)$, in which the C−H bond of methane is activated, Rh(I) is oxidized to Rh(III), and methane is cleaved. Quantum zero point energy is included in 39 vibrational modes, excited vibrational states are also quantized, and quantum mechanical tunneling contributions are included by the multidimensional small-curvature tunneling approximation. Born−Oppenheimer potential energies, reaction-path geometries, and vibrational frequencies needed for the rate calculations are obtained from density functional theory using the direct dynamics approach. At 200 K the rate constant calculated with quantum effects is 194 times larger than the rate constant calculated using classical mechanics to describe the atomic motion. Including quantized vibrational energies but not tunneling reduces this discrepancy to a factor of 3.4. These factors are increased to 2770 and 11 at 150 K and decreased to 20 to 1.67 at 300 K. Thus the effect of quantizing vibrations is greater than 1 order of magnitude over this entire temperature range.

1. Introduction

Catalytic cycles involving the oxidation and reduction of transition-metal complexes can be used for selective functionalization of hydrocarbons through C−H bond activation.[1] Due to the fundamental economic importance of such processes, substantial experimental[1−12] and theoretical[13−20] effort has been put into understanding them. It has been found that iridium(I) and rhodium(I) complexes are the most useful for activation of C−H bonds.

Scheme 1

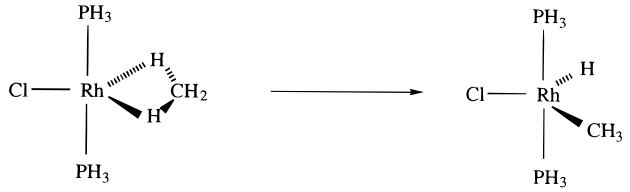

Reactant **1** Product **2**

In this work, we studied the reaction path for a unimolecular rearrangement, shown in Scheme 1, involving the oxidative cleavage of methane, initially in a η^2 adduct of a Rh complex. The analogous reaction in which PH_3 is replaced by $P(CH_3)_3$ and CH_4 is replaced by a more general alkane is a part of the complete catalytic cycle for C−H bond functionalization developed by Sakakura and Tanaka.[8]

Previous theoretical studies of the reaction path for such oxidative cleavage reactions have been very informative. Koga and Morokuma[15] performed electronic structure calculations on a rhodium-based C−H activation reaction, and they found that the reaction proceeds through a bifurcated η^2 complex like **1**, in agreement with the experimental suggestion of Periana and Bergman.[7] Later, Blomberg *et al.*[16] performed calculations for the oxidative addition reactions between methane and the whole sequence of second row transition metal atoms from yttrium to palladium. For the rhodium system they found that the same η^2 complex is less stabilized and the reaction is more endothermic. Margl *et al.*[19] also calculated the stationary points (reactant η^2 adduct, transition state, and product hydridoalkylrhodium complex) of interest here and obtained an energy of reaction intermediate between the two values of the earlier works. Although the precise energetic parameters are strongly dependent of the level of calculation, the insight one can obtain

† Visiting scientist, Spring 1997. Current address: Departamento de Química Física, Universidad de Extremadura, 06071 Badajoz, Spain.

⊗ Abstract published in *Advance ACS Abstracts,* October 1, 1997.

(1) Tanaka, M.; Sakakura, T. In *Advances in Chemistry Series*; Moser, W. R., Slocum, D. W., Eds.; American Chemical Society: Washington, D.C., 1992; Vol. 230, p 181.
(2) Janowicz, A. H.; Bergman, R. G. *J. Am. Chem. Soc.* **1982**, *104*, 352.
(3) (a) Hoyano, J. K.; Graham, W. A. G. *J. Am. Chem. Soc.* **1982**, *104*, 3724. (b) Rest, A. J.; Whitwell, I.; Graham, W. A. G.; Hoyano, J. K.; McMaster, A. D. *J. Chem. Soc., Chem. Commun.* **1984**, 624.
(4) Jones, W. D.; Feher, F. J. *J. Am. Chem. Soc.* **1982**, *104*, 4240; **1986**, *108*, 4814.
(5) Shilov, A. E. *Activation of Saturated Hydrocarbons*; Reidel: Dordrecht, 1984.
(6) (a) Crabtree, R. H. *Chem. Rev.* **1985**, *85*, 245. (b) Crabtree, R. H.; Holt, E. M.; Lavin, M.; Morehouse, S. M. *Inorg. Chem.* **1985**, *24*, 1986. (c) Crabtree, R. H. *Angew. Chem., Int. Ed. Engl.* **1993**, *32*, 289.
(7) Periana, R. A.; Bergman, R. G. *J. Am. Chem. Soc.* **1986**, *108*, 7332.
(8) Sakakura, T.; Tanaka, M. *Chem. Lett.* **1987**, *249*, 1113.
(9) Jones, W. D.; Feher, F. J. *Acc. Chem. Res.* **1989**, *22*, 91.
(10) Sakakura, T.; Sodeyama, T.; Sakaki, K.; Wada, K.; Tanaka, M. *J. Am. Chem. Soc.* **1990**, *112*, 7221.
(11) Wasserman, E. P.; Morse, C. B.; Bergman, R. G. *Science* **1992**, *255*, 315.
(12) (a) Arndtsen, B. A.; Bergman, R. G.; Mobley, T. A.; Peterson, T. H. *Acc. Chem. Res.* **1995**, *28*, 154. (b) Purwoko, A. A.; Lees, A. J. *Inorg. Chem.* **1996**, *35*, 675. (c) Paneque, M.; Taboada, S.; Carmona, E. *Organometallics* **1996**, *15*, 2678. (d) Osakada, K.; Koizumi, T.; Yamamoto, T. *Bull. Chem. Soc. Jpn.* **1997**, *70*, 189.
(13) Saillard, J.-Y.; Hoffmann, R. *J. Am. Chem. Soc.* **1984**, *106*, 2006.
(14) (a) Low, J. J.; Goddard, W. A. III. *J. Am. Chem. Soc.* **1984**, *106*, 8321. (b) Ziegler, T.; Tschinke, V.; Fan, L.; Becke, A. D. *J. Am. Chem. Soc.* **1989**, *111*, 9177.
(15) Koga, N.; Morokuma, K. *J. Phys. Chem.* **1990**, *94*, 5454.
(16) Blomberg, M. R. A.; Siegbahn, P. E. M.; Svensson, M. *J. Am. Chem. Soc.* **1992**, *114*, 6095.
(17) Song, J.; Hall, M. B. *Organometallics* **1993**, *12*, 3118.
(18) (a) Siegbahn, P. E. M.; Svensson, M. *J. Am. Chem. Soc.* **1994**, *116*, 10124. (b) Siegbahn, P. E. M. *Theor. Chim. Acta* **1994**, *87*, 277.
(19) Margl, P.; Ziegler, T.; Blöchl, P. E. *J. Am. Chem. Soc.* **1995**, *117*, 12625.
(20) Su, M.-D.; Chu, S.-Y. *J. Am. Chem. Soc.* **1997**, *119*, 5373.

S0002-7863(97)02209-9 CCC: $14.00

into the dynamics need not be so limited. Margl *et al.*[19] also reported dynamics simulations based on classical mechanics[21] for the atomic motions, and the goal of the present work is to elucidate the role of quantum effects in the dynamics.

The validity of the dynamical conclusions about a chemical reaction depends on the method used to simulate the dynamics. The model reaction studied here has 45 degrees of freedom, and like Margl *et al.*,[19] we use the direct dynamics approach,[21−24] in which the dynamics calculations are based directly on electronic structure calculations of the energy and energy derivatives without the intermediacy of an analytic potential energy function or force field. In the present work we use a reaction-path direct dynamics method in which electronic structure calculations are required only in the region of the configuration space lying along the reaction path. In particular, we calculate the minimum energy path[25] (MEP) for the rearrangement of Scheme 1 and the reaction valley formed by the motions orthogonal to the reaction path. This data is used to calculate the reaction rate both classically and also with inclusion of quantum effects.

2. Theory

All coordinates are scaled by $(m_A/\mu)^{1/2}$, where m_A is the mass of the atom to which a given coordinate corresponds, and μ is 1 amu, because, as is well-known,[26] this simplifies the interpretation of vibrational motions. The reaction coordinate s is defined as the signed distance along the MEP, through mass-scaled coordinates, and the generalized normal-mode coordinates at a given point along the MEP[27] are denoted $Q_m(s)$, where $m = 1, 2, ..., 3N - 7$, and N is the number of atoms. The momenta conjugates to s and $Q_m(s)$ are denoted P_s and P_m, respectively. The leading terms in the Hamiltonian in the vicinity if the MEP are[28]

$$H = \frac{1}{2\mu}\left[\frac{Ps}{1 + \sum_{m=1}^{3N-7} Q_m(s)B_{mF}(s)}\right]^2 + T_{rot}(J_{cl},s) + V_{MEP}(s) + \frac{1}{2}\sum_{m=1}^{3N-7}\left\{\frac{P_m^2}{\mu} + \mu[\omega_m(s)Q_m(s)]^2\right\} \quad (1)$$

where $V_{MEP}(s)$ is the Born-Oppenheimer potential energy along the MEP, B_{mF} is the reaction-path curvature in mode m, $\omega_m(s)$ is a generalized normal-mode vibrational frequency, and $T_{rot}(J_{cl},s)$ is the rotational kinetic energy for angular momentum J_{cl}. The total reaction-path curvature is

$$\kappa(s) = (\sum[B_{mF}(s)]^2)^{1/2} \quad (2)$$

Using eq 1, we calculated rate constants by variational transition state theory, in particular canonical variational theory, by finding the maximum free energy of activation as a function of s.[27] This corresponds to calculating the one-way flux through the variationally optimized dynamical bottleneck. Quantum effects on reaction coordinate motion are included by the multidimensional small-curvature tunneling approximation, which takes into account corner-cutting of the tunneling path through vibrational degrees of freedom with nonzero curvature coupling, $B_{mF}(s)$, to the reaction coordinate.[24] These dynamical treatments have been validated against complete quantum dynamics calculations in earlier work.[29]

We distinguish three levels for including (or neglecting) quantum effects:

(1) classical: Vibration is treated classically, and tunneling is neglected.

(2) hybrid: Vibration is treated quantum mechanically, but tunneling is still neglected.

(3) quantal: Vibration is treated quantum mechanically, and tunneling is included.

3. Computational Details

Although Margl *et al.*[19] calculated for this system that the conformation of the adduct with phosphine groups *cis* to each other is more stable than the *trans* one, we carried out rate calculations for the *trans* conformation because it is closer to the experimental situation.

Geometries, energies, and first and second energy derivatives were calculated by density functional theory (DFT)[30] using the GAUSSIAN 94[31] system of programs. Exchange and correlation were treated by

(21) (a) Parrinello, M. In *Modern Techniques in Computational Chemistry*; Clementi, E., Ed.; ESCOM: Leiden, 1991; pp 833−845. (b) Galli, G.; Parrinello, M. In *Computer Simulations in Material Science*; Kluwer: Dordrecht, 1991; pp 283−304.

(22) (a) Wang, I.; Karplus, M. *J. Am. Chem. Soc.* **1973**, *95*, 8160. (b) Malcome-Lawes, D. J. *J. Chem. Soc., Faraday Trans. II* **1975**, *71*, 1183. (c) Warshel, A.; Karplus, M. *Chem. Phys. Lett.* **1975**, *32*, 11. (d) Leforestier, C. *J. Chem. Phys.* **1978**, *68*, 4406. (e) Morokuma, K.; Kato, S. In *Potential Energy Surfaces and Dynamics Calculations*; Truhlar, D. G., Ed.; Plenum: New York, 1981; p 243. (f) Truhlar, D. G.; Duff, J. W.; Blais, N. C.; Tully, J. C.; Garrett, B. C. *J. Chem. Phys.* **1982**, *77*, 764. (g) Car, R.; Parrinello, M. *Phys. Rev. Lett.*, **1985**, *55*, 2471. (h) Tachinaba, A.; Ukazaki, I.; Koizumi, M.; Hori, K.; Yomabe, T. *J. Am. Chem. Soc.* **1985**, *107*, 1190. (i) Colwell, S.; Handy, N. C. *J. Chem. Phys.* **1985**, *82*, 1281.

(23) (a) Doubleday, C. J.; McIver, J. W., Jr.; Page, M. *J. Chem. Phys.* **1988**, *92*, 4367. (b) Baldridge, K. M.; Gordon, M. S.; Steckler, R.; Truhlar, D. G. *J. Phys. Chem.* **1989**, *93*, 5107; (c) Truhlar, D. G.; Gordon, M. S. *Science* **1990**, *249*, 491. (d) Helgaker, T.; Uggerud, E.; Jensen, H. J. A. *Chem. Phys. Lett.* **1990**, *173*, 145. (e) Liu, Y.-P.; Lu, D.-h.; Gonzalez-Lafont, A.; Truhlar, D. G.; Garrett, B. C. *J. Am. Chem. Soc.* **1993**, *115*, 7806, and references therein. (f) Page, M. *Comput. Phys. Commun.* **1994**, *84*, 115. (g) Truhlar, D. G. In *The Reaction Path in Chemistry*; Heidrich, D., Ed.; Kluwer: Dordrecht, 1995; p 229. (h) Truong, T. N.; Duncan, W. T.; Bell, R. L. *ACS Symp. Ser.* **1996**, *629*, 85.

(24) Liu, Y. P.; Lynch, G. C.; Truong, T. N.; Lu, D.-h.; Truhlar, D. G. *J. Am. Chem. Soc.* **1993**, *115*, 2408.

(25) (a) Marcus, R. A. *J. Chem. Phys.* **1966**, *45*, 4493. (b) Truhlar, D. G.; Kuppermann, A. *J. Am. Chem. Soc.* **1970**, *93*, 1840. (c) Fukui, K. *Pure Appl. Chem.* **1982**, *54*, 1825.

(26) Wilson, E. B., Jr.; Decius, J. C.; Cross, P. C. *Molecular Vibrations*; McGraw-Hill: New York, 1955.

(27) (a) Garrett, B. C.; Truhlar, D. G. *J. Chem. Phys.* **1979**, *70*, 1593. (b) Truhlar, D. G.; Isaacson, A. D.; Garrett, B. C. In *The Theory of Chemical Reactions*; Bear, M., Ed.; Chemical Rubber: Boca Raton, FL, 1985; Vol. 4.

(28) (a) Miller, W. H.; Handy, N. C.; Adams, J. E. *J. Chem. Phys.* **1980**, *72*, 99. (b) For the special case with $m_{max} = 1$, see: Marcus, R. A. *J. Chem. Phys.* **1966**, *45*, 4500. Equation 1 neglects rotation−vibration coupling, curvilinear effects on the harmonic frequencies, anharmonicity, and curvature-induced coupling of the generalized normal modes, all of which have been discussed elsewhere in the literature; see ref 28a and (c) Garrett, B. C.; Truhlar, D. G. *J. Phys. Chem.* **1979**, *83*, 1915. (d) Miller, W. H. In *Potential Energy Surfaces and Dynamics Calculations*; Truhlar, D. G. Ed.; Plenum: New York, 1981; p 265. (e) Isaacson, A. D.; Truhlar, D. G. *J. Chem. Phys.* **1982**, *76*, 1380. (f) Garrett, B. C.; Truhlar, D. G. *J. Chem. Phys.* **1984**, *81*, 309. (g) Liu, Y.-P.; Lu, D.-h.; Gonzalez-Lafont, A.; Truhlar, D. G.; Garrett, B. C. *J. Am. Chem. Soc.* **1993**, *115*, 7806. (h) Jackels, C. F.; Gu, Z.; Truhlar, D. G. *J. Chem. Phys.* **1995**, *102*, 3188. On the basis of these studies it seems unlikely that inclusion of these higher-order terms would change the conclusions of this paper.

(29) Truhlar, D. G.; Garrett, B. C.; Klippenstein, S. J. *J. Phys. Chem.* **1996**, *100*, 12771.

(30) (a) Parr, R. G.; Yang, W. In *Density Functional Theory of Atoms and Molecules*; Oxford University Press: New York, 1989. (b) Ziegler, T. *Chem. Rev.* **1991**, *91*, 651.

(31) GAUSSIAN 94. Frisch, M. J.; Trucks, G. W.; Schlegel, H. B.; Gill, P. M. W.; Johnson, B. G.; Robb, M. A.; Cheeseman, J. R.; Keith, T.; Petersson, G. A.; Montgomery, J. A.; Raghavachari, K.; Al-Laham, M. A.; Zakrzewski, V. G.; Ortiz, J. V.; Foresman, J. B.; Ciolowski, J.; Stefanov, B. B.; Nanayakkara, A.; Challacombe, M.; Peng, C. Y.; Ayala, P. Y., Chen, W.; Wong, M. W.; Andres, J. L.; Replogle, E. S.; Gomperts, R.; Martin, R. L.; Fox, D. J.; Binkley, J. S.; Defrees, D. J.; Baker, J.; Stewart, J. P.; Head-Gordon, M.; Gonzalez, C.; Pople, J. A. Gaussian Inc., Pittsburgh, 1995.

the B3LYP method,[32] which is based on Becke's three-parameter hybrid method[33] for combining Hartee−Fock exchange with a local-density-approximation exchange-correlation functional,[34] Becke's 1988 gradient-corrected exchange functional (B88),[35] and the gradient-corrected correlation functional of Lee, Yang, and Parr.[36] Dynamics calculations were carried out by a dual-level[37−39] scheme. For the low level, we use the LANL2DZ basis set, which involves a valence double-ζ basis[40] on C and H and the Los Alamos effective core potential (ECP) with a double-ζ basis[41] for P, Cl, and Rh. For the higher level we used a larger basis set, namely, 3-21G(d,p)[42] for rhodium and 6-311G(d,p)[43] for the rest of atoms, which yields 192 basis functions.

We initiated the reaction path by following the imaginary-frequency mode of the saddle point in both downhill directions toward reactants and products, and we propagated it using the method of Gonzalez and Schlegel,[44] with a step size of 0.05 Å, out to a distance of 0.80 Å on both sides of the saddle point. In this process one must be careful that the electronic structure algorithms do not reorient the molecule. The frequencies $\omega_m(s)$ and reaction-path curvature components were computed at a total of 19 geometries along the reaction path. Frequencies at nonstationary points were computed by the usual method of projecting out the local rectilinear reaction-coordinate motion.[28a,d,e,g] The information between the points at $s = -0.80$ Å and reactants (estimated to be located at $s = -2.7$ Å) and $s = 0.80$ Å and products (estimated to be located at $s = 1.9$ Å) was interpolated by using third-order Lagrangian interpolation. The same procedure was used for interpolating the information between two consecutive points along the reaction path. We checked that adiabatic and diabatic interpolation of frequencies at narrowly avoided crossings give essentially the same rate constants.

The energy along the reaction path was corrected using the single-point energies calculated for the stationary points with the larger basis, according to the procedure described elsewhere[37] for unimolecular reactions.

As a consequence of the flatness of the potential energy surface, a tight convergence criterion and a certain amount of manual geometry perturbation in modes with negative force constants were required to converge to the correct structures. The nature of all stationary points was verified by Hessian analysis, which showed $3N - 6$ real frequencies for minima and $3N - 7$ real frequencies and one imaginary frequency for the saddle point. The low values of some of the vibrational frequencies quantify the flatness of the potential energy surface with respect to some of the internal motions in the reactant, saddle point, and product. (This is the first time that such vibrational analysis and stationary point classification has been carried out for this large, floppy system.)

Rate constants were calculated as explained in Section 2. Temperature-dependent Arrhenius activation energies were calculated from the rate constants as local slopes of conventional Arrhenius plots. All dynamics calculations were carried out with the general polyatomic rate constant code POLYRATE.[45]

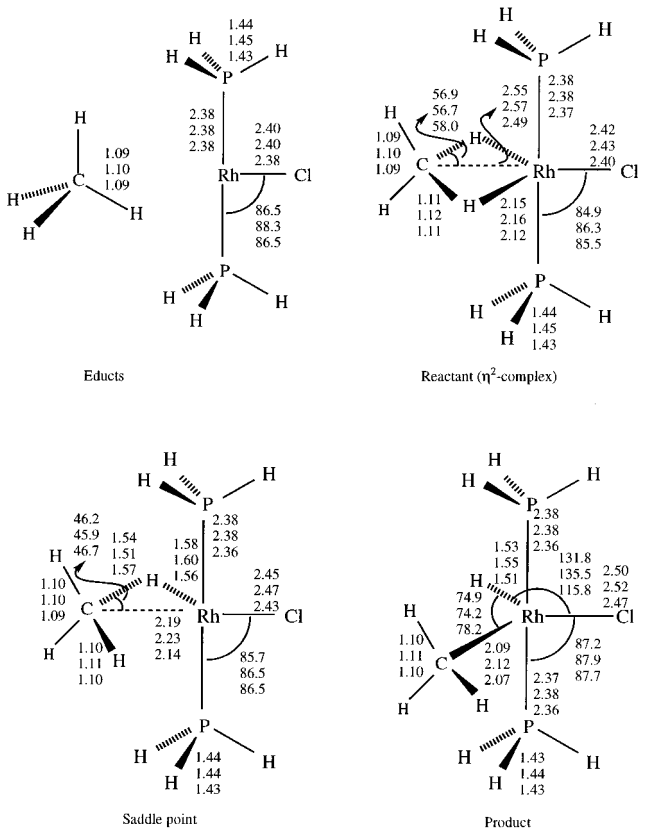

Figure 1. Optimized geometries (in angstroms and degrees) for the three stationary points and the educts. For each bond distance or angle, the first row corresponds to the B3LYP level, the second to the B88LYP level, and the third to the BHHLYP level. All these calculations used the LANL2DZ basis set.

4. Results and Discussion

4.1. Stationary Points. Since saddle points may be particularly sensitive to the treatment of electron exchange,[46] we optimized the stationary point geometries with three different exchange functionals, namely B3,[32,33] B88,[35] and Becke's half-and-half method[47] (BHH), which is a 50:50 hybrid of B88 and Hartree−Fock exchange. Figure 1 shows the optimized geometries of the stationary points and the educts at the three levels of calculation: B3LYP, B88LYP, and BHHLYP. In general, the three levels yield similar geometries, with very small differences in distances and angles, and they agree with earlier theoretical geometries optimized using different levels and basis sets.[15,16,19] The similarities of results with different levels confirms that the B3LYP/LANL2DZ level is reasonable for geometries. At this level, the η^2 complex has a Rh−C distance of 2.55 Å, and the C−H bonds directly involved in complexation and the Rh−Cl bond have the largest variations (0.02 Å) from the educts. The other bond lengths and bond angles are very close to those of the educts. The C−Rh−Cl bond angle is linear.

At the transition state one of the H−Rh distances has decreased from 2.12−2.16 to 1.56−1.60 Å, while the other one has increased from 2.12−2.16 to 2.45−2.49 Å. The transition

(32) Stephens, P. J.; Devlin, F. J.; Chabalowski, C. F.; Frisch, M. J. *J. Phys. Chem.* **1994**, *98*, 11623.
(33) Becke, A. D. *J. Chem. Phys.* **1993**, *98*, 5648.
(34) (a) Slater, J. C. *Adv. Quantum Chem.* **1972**, *6*, 1. (b) Vosko, S. H.; Wilk, L.; Nusair, M. *Can. J. Phys.* **1980**, *58*, 1200.
(35) Becke, A. *Phys. Rev. A* **1988**, *38*, 3098.
(36) Lee, C.; Yang, W.; Parr, R. G. *Phys. Rev. B* **1988**, *37*, 785.
(37) Hu, W.-P.; Liu, Y.-P.; Truhlar, D. G. *J. Chem. Soc., Faraday Trans.* **1994**, *90*, 1715.
(38) Corchado, J. C.; Espinosa-García, J.; Hu, W.-P.; Rossi, I.; Truhlar, D. G. *J. Phys. Chem.* **1995**, *99*, 687.
(39) Linder, D. P.; Duan, X.; Page, M. *J. Chem. Phys.* **1996**, *104*, 6298.
(40) Dunning, T. H.; Hay, P. J. In *Modern Theoretical Chemistry*; Schaefer, H. F., Ed.; Plenum: New York, 1977; Vol. 2, pp 1−28.
(41) (a) Hay, P. J.; Wadt, W. R. *J. Chem. Phys.* **1985**, *82*, 270. (b) Wadt, W. R.; Hay, P. J. *J. Chem. Phys.* **1985**, *82*, 284.
(42) Pietro, W. J.; Francl, M. M.; Hehtr, W. J.; Defrees, D. J.; Pople, J. A.; Binkley, J. S. *J. Am. Chem. Soc.* **1982**, *104*, 5039.
(43) (a) Krishnan, R.; Binkley, J. S.; Seeger, R.; Pople, J. A. *J. Chem. Phys.* **1980**, *72*, 650. (b) McLean, A. D.; Chandler, G. S. *J. Chem. Phys.* **1980**, *72*, 5639.
(44) Gonzalez, C; Schlegel, H. B. *J. Chem. Phys.* **1989**, *90*, 2154.
(45) Steckler, R.; Chuang, Y. Y.; Coitiño, E. L.; Fast, P. L.; Corchado, J. C.; Hu, W.-P.; Liu, Y.-P.; Lynch, G. C.; Nguyen, K. A.; Jackels, C. F.; Gu, M. Z.; Rossi, I.; Clayton, S.; Melissas, V. S.; Garrett, B. C.; Isaacson, A. D.; Truhlar, D. G. POLYRATE, Version 7.2, University of Minnesota, Minneapolis, 1997.
(46) (a) Baker, J.; Andzelm, J.; Muir, M.; Taylor, P. R. *Chem. Phys. Lett.* **1995**, *236*, 53. (b) Skokov, S.; Wheeler, R. A. *Chem. Phys. Lett.* **1997**, *221*, 251.
(47) Becke, A. *J. Chem. Phys.* **1993**, *98*, 1372.

Table 1. Five Lowest Vibrational Frequencies and Relative Molar Energies and Enthalpies of Stationary Points[a,b]

	ω_m (cm^{-1})	ΔE (kcal)	ΔH_0^0 (kcal)
educts[b]	73, 73, 80, 111, 122	15.1[c]	13.9
reactant	65, 89, 93, 108, 110	0.0	0.0
saddle point	78, 97, 103, 111, 121	8.8[d]	6.9
product	43, 86, 90, 98, 106	4.7[e]	3.5

[a] ΔE is the Born−Oppenheimer energy difference; ΔH_0^0 is the enthalpy change, including zero point energy, at 0 K. ΔH_0^0 for the saddle point is actually the enthalpy of activation, i.e., the imaginary-frequency mode is omitted. [b] There are three candidates for the ground state of the $Rh(PH_3)_2Cl$ educt: closed-shell singlet, $(a_2)^2\,(b_1)^2\,(b_2)^2\,(1a_1)^2$, $^1A_1$; open-shell singlet, $(a_2)^2\,(b_1)^2\,(b_2)^2\,(1a_1)^1\,(2a_1)^1$, $^1A_1$; and open-shell triplet, $(a_2)^2\,(b_1)^2\,(b_2)^2\,(1a_1)^1\,(2a_1)^1$, $^3A_1$. Koga and Morokuma[15] and Blomberg *et al.*[16] calculated that the triplet is the ground state, but Margl *et al.*[19] found the closed-shell singlet to be of lowest energy. With the smaller basis, we performed a comparison between the closed-shell singlet and the open-shell triplet and found the triplet to be lower in energy but by only 0.75 kcal mol^{-1}. Since the splitting between the singlet and the triplet state is very small, the order of stability depends on the level of calculation. However, since the reaction path follows a closed-shell singlet route, we consider only the singlet state here and in the rest of the paper. [c] Previous values[15,16,19] are 12−18. [d] Previous values[15,16,19] are 3−10. [e] Previous values[15,16,19] are −7 to +2.

structure is a three-centered (C−H−Rh) structure, where the length of the bond that is broken (C−H) is increased by about 40% from 1.11−1.12 to 1.52−1.57 Å, and the lengths of the bonds that are formed (Rh−H and Rh−C) are elongated by only 3% and 5%, respectively, with respect to their values in the product. Since the reaction is endothermic (see below), this is the behavior expected according to the Hammond postulate,[48] with the saddle point being closer to products than to reactants. This is also in agreement with our estimated mass-scaled distances along the reaction path between the saddle point and reactants (2.7 Å) and saddle point and products (1.9 Å). The saddle point has an imaginary frequency of 808i cm^{-1}. This value is related to the mass-scaled width of the potential energy barrier along the MEP and, therefore, to the magnitude of the tunneling effect.

The five lowest harmonic frequencies for each stationary point are given in Table 1 to illustrate the smallness of the low frequencies associated with bending and torsion motions and hence the flat character of the potential energy surface. The energy and enthalpy changes (reaction and activation) along the reaction path are also presented in Table 1. The energies are similar to earlier[15,16,19] theoretical results.

4.2. Reaction Path and Reaction Valley. The main focus of the present work is the analysis of the reaction path, reaction valley, and dynamics.

Figure 2 shows the making and breaking bond distances, R(Rh−H) and R(C−H), as functions of the reaction coordinate, s. As the reaction proceeds, the breaking C−H bond remains practically constant until about 0.4 Å before the saddle point, where it begins to change linearly. The change in the forming Rh−H bond proceeds more gently, and it is almost complete by about 0.1 Å after the saddle point. Thus the concerted portion of the reaction path is only about 0.5 Å wide.

The reaction path curvature, $\kappa(s)$ in eq 2, is shown as a function of s in Figure 3. There are two significant peaks in the entrance channel and one in the exit channel. The former are due to strong coupling between the CH_4 bending modes (peak at $s \approx -0.5$ Å) and the reaction coordinate and between the stretching mode of the breaking C−H bond and the reaction coordinate (peak at $s \approx -0.4$ Å). In fact, the curvature in the breaking C−H bond coordinate at $s \approx -0.4$ Å was also seen in Figure 2. Since it has been shown that peaks in the curvature

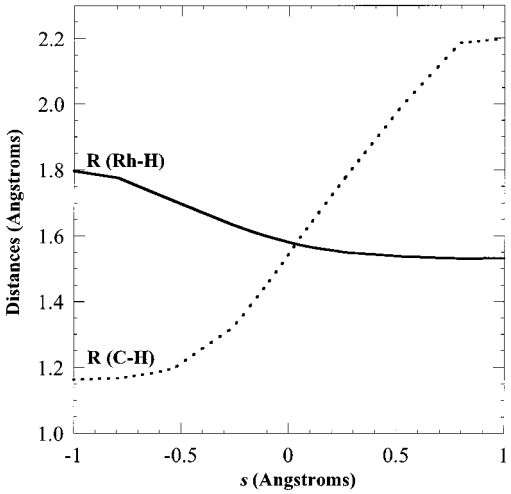

Figure 2. Bond distances between Rh and the cleaved H (solid curve) and between C and the bridging H that is retained by the methyl group (dashed curve) as functions of the reaction coordinate, s. Note that $s = 0$ corresponds to the saddle point.

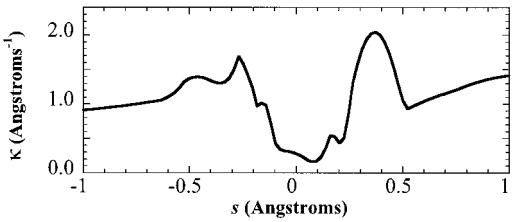

Figure 3. Curvature of the reaction path as a function of the reaction coordinate.

coupling correlate with energy transfer between the reaction coordinate and transverse motions,[28b,49] this peak shows where energy can flow nonadiabatically from the CH_4 bending modes into the reaction coordinate, and thus the present calculations predict that vibrational excitation of CH_4 bending modes and C−H stretches can increase the rate constant. The peak in the exit channel is due to strong coupling between the C−H stretch, CH_3 bending, and the reaction coordinate. Therefore, we predict that the CH_3 bending modes will be excited in the nascent product.

Some of the 38 vibrational frequencies along the MEP are shown in Figure 4. The degrees of freedom can be separated into two types: spectator modes and modes involving making and breaking bonds. The spectator modes are those basically unchanged in going from reactants to the transition state, and they are related to motions which are not directly involved in the reaction. Examples are the two C−H stretching modes not directly involved in the reaction, the six P−H stretching modes, and the PH_3 bending modes. The lowest-frequency modes, not plotted in Figure 5, correspond to bending motions and torsions associated with to the relative motions of methane and $Rh(PH_3)_2$-Cl. These modes are related to the weak interaction that binds the complex and hence are low-frequency modes. Two modes are directly involved in the hydrogen transfer and correspond to a C−H stretching mode at the reactant complex (2684 cm^{-1}), and the Rh−H stretch mode (2204 cm^{-1}) at the product. The frequencies of these modes show an avoided crossing (1:1 resonance) at about $s \approx -0.5$ Å and show the largest variations along the reaction path.

(48) Hammond, G. S. *J. Am. Chem. Soc.* **1955**, *77*, 334.

(49) (a) Marcus, R. A. *J. Chem. Phys.* **1968**, *49*, 2610. (b) Hofacker, G. L.; Levine, R. D. *Chem. Phys. Lett.* **1973**, *15*, 165, **1975**, *33*, 404. (c) Hofacker, G. L.; Michel, K. W. *Ber. Busenges. Physik. Chem.* **1974**, *28*, 124. (d) Ben-Shaul, A.; Hofacker, G. L. In *Handbook of Chemical Lasers*; Gross, R. F. W., Bott, J. F., Eds.; Wiley-Interscience: New York, 1976; p. 529. (e) Duff, J. W.; Truhlar, D. G. *J. Chem. Phys.* **1975**, *62*, 2477.

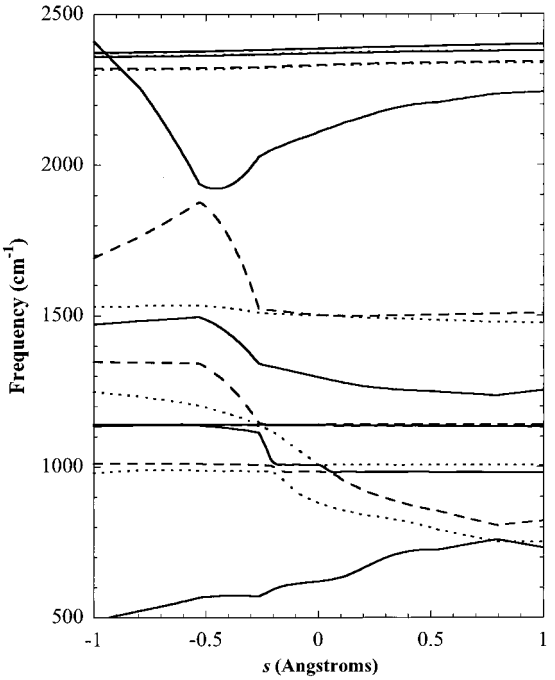

Figure 4. Vibrational frequencies in the interval 500−2500 cm^{-1} plotted versus the reaction coordinate.

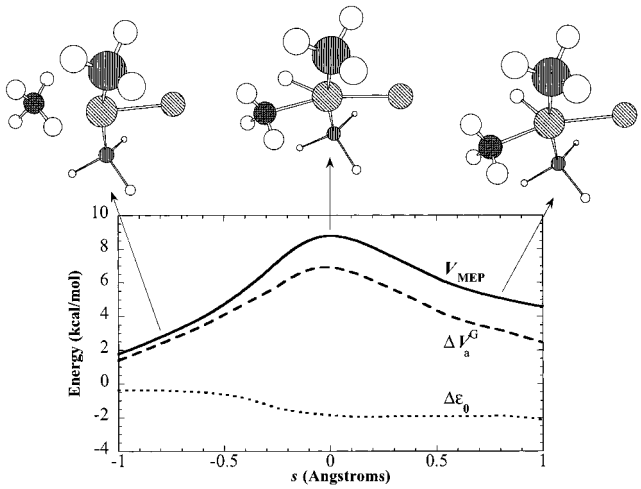

Figure 5. Born−Oppenheimer potential energy relative to reactants (V_{MEP}), total zero-point energy relative to reactants ($\Delta\epsilon_0$), and vibrationally adiabatic potential energy curve relative to reactants (ΔV_a^G) as functions of s. The structures at three points along the MEP (s = −0.8, 0.0, and +0.8 Å) are illustrated above the plot.

The potential energy along the MEP, the change in local zero point energy of transverse modes, $\Delta\epsilon_0(s)$, and the relative ground-state vibrationally adiabatic curve, ΔV_a^G, are plotted as functions of s in Figure 5. The latter curve is defined by

$$\Delta V_a^G(s) = V_{MEP}(s) + \Delta\epsilon_0(s) \qquad (3)$$

and it is important for two reasons. First, it provides the effective potential for tunneling,[25a,b,50] and, second, except for an additive constant, it is the same as the free energy of activation profile at 0 K and similar to and illustrative of the finite-temperature free energy of activation profiles.[51] The ΔV_a^G profile is somewhat flatter near the top than the V_{MEP} profile, and the maximum is slightly shifted to $s = -0.02$ Å. The barrier heights of the V_{MEP} and ΔV_a^G curves are, respectively, 8.8 and 6.9 kcal/mol relative to their respective values at **1**.

Table 2. Calculated Rate Constants (s^{-1})

T (K)	classical	hybrid	quantal
150	9.66(−1)[a]	2.51(2)	2.68(3)
175	6.46(1)	7.07(3)	3.72(4)
200	1.51(3)	8.56(4)	2.93(5)
225	1.75(4)	5.92(5)	1.53(6)
250	1.24(5)	2.76(6)	5.89(6)
275	6.17(5)	9.72(6)	1.80(7)
300	2.35(6)	2.77(7)	4.63(7)

[a] 4.34(3) denotes 4.34 × 10^3.

4.3. Rate Constant Calculations. Table 2 lists the calculated rate constants for the temperature range 150−300 K. For perspective we note that the typical temperature for the experiments of ref 7 was 213 K, near the center of our range.

The quantal and classical descriptions of the system yield very different vibrational contributions to the rate constant, especially for the higher-frequency modes. In the absence of frequency changes along the reaction path, neglecting the quantization of vibrational energy at the reactant would cancel the effect of such neglect at the dynamical bottleneck. However, even though we are studying an intramolecular rearrangement, the present calculations show a significant change in the vibrational frequencies along the reaction path. The change in the frequencies along the reaction path leads to very different results for the classical and hybrid rate calculations. Thus, the classical description underestimates the hybrid rate constants by factors ranging from 260 to 12 over the temperature range from 150 to 300 K. These results show that classical mechanical simulation of the type now becoming very popular[21,52] are not suitable for studying this problem. The classical calculations lead to an essentially linear Arrhenius plot over the whole temperature range under study with an activation energy, E_a, of 8.8 kcal/mol.

Tunneling effects are very significant, increasing the rate constant by a factor of 1.8 at 300 K, 4.3 at 200 K, and 17 at 150 K. Oxidative coordination reactions of CH_4 have been observed at temperatures as low as 12 K,[3b] and quantum effects are expected to be even larger under such conditions. At 200 K, the most probable tunneling energy[53] is 0.51 kcal/mol below the top of the ground-state vibrationally adiabatic barrier; at this energy the tunneling path extends from $s = -0.17$ Å to $s = +0.15$ Å. The dominant curvature couplings occur both before and after this range (see Figure 3), and so curvature effects on the magnitude of the tunneling contribution turn out to be important only in a quantitative sense, but do not change the results qualitatively. Thus, at 200 K, corner cutting effects increase the tunneling rate by only 16% as compared to tunneling along the MEP. Nevertheless, these effects are fully included in the quantal results of Table 2.

An important qualitative feature in systems dominated by tunneling processes is that they often show a temperature-

(50) Skodje, R. T.; Truhlar, D. G.; Garrett, B. C. *J. Chem. Phys.* **1982**, *77*, 5955 and references therein.

(51) Garrett, B. C.; Truhlar, D. G. *J. Am. Chem. Soc.* **1979**, *101*, 4534.

(52) (a) Nagaoka, M.; Okuko, Y.; Yamabe, T. *J. Phys. Chem.* **1994**, *98*, 12506. (b) Meier, R. J.; van Doremaele, G. H. J.; Iarlori, S.; Buda, F. *J. Am. Chem. Soc.* **1994**, *116*, 7274. (c) van Doremaele, G. H. J.; Meier, R. J.; Iarlori, S.; Buda, F. *J. Mol. Struct. (THEOCHEM)* **1996**, *363*, 269. (d) For a recent review of classical trajectory methods, including quasiclassical corrections, see: Sewell, T. D.; Thompson, D. L. *Int. J. Mod. Phys. B* **1997**, *11*, 1067.

(53) Kim, Y.; Truhlar, D. G.; Kreevoy, M. M. *J. Am. Chem. Soc.* **1991**, *113*, 7837.

dependent Arrhenius activation energy.[54] Our results for the temperature intervals 150−175, 200−225, and 275−300 K are 5.5, 5.9, and 6.2 kcal/mol. The importance of tunneling in this reaction is responsible not only for this temperature variation but also for the fact that the activation energies are lower than both the classical and vibrationally adiabatic barrier heights. The Arrhenius E_a is about 3 kcal/mol below the classical barrier height. This new information about the temperature dependence of phenomenological activation energies and their relation to barrier height should be useful for future attempts to infer barrier heights from experiment.

There are no experimental data for comparison to the calculated rate constants, but comparison of absolute rate constants to experiment is not the point of this study. Rather we are interested in elucidating the role of quantum effects on the dynamics and kinetics. Furthermore, if experimental rates were available, it is unlikely that the absolute rates would be predicted quantitatively because of the difficulty in predicting absolute barrier heights by electronic structure theory.[13−20,29,46]

The conclusion that zero point effects must be added to molecular dynamics simulation of organometallic reactions was also pointed out (for a different system) by Margl *et al.*[55] although the effect of quantization does not appear in their classical treatment[21] of the dynamics. In general it is difficult to add quantization effects to classical simulations of dynamics because the zero point energy quantization effects must be added at the dynamical bottleneck,[56] but zero point energy placed in high-frequency modes tends to drain into other motions in a nonphysical way.[57] Furthermore, dynamical bottlenecks occur at a variety of locations in configuration space.[58] Canonical variational theory provides a reasonable compromise by locating the bottleneck where it minimizes the reactive flux averaged over a canonical ensemble.[27] Furthermore the incorporation of vibrational quantization effects in canonical variational theory is efficient. The other quantum effect included in this work is tunneling, and this appears to be the first calculation of tunneling contributions to an organometallic reaction in which all degrees of freedom are included. Accurate quantal dynamics calculations confirm the essential correctness of quantizing vibrational energies at dynamical bottlenecks and the broadening of thresholds by tunneling.[58k,59]

The present study has focused on the rate constant for the elementary reaction step of Scheme 1. This may or may not be the analog of the rate-determining step in an overall catalytic cycle or synthetic procedure, depending upon the system, the conditions, and the possible presence of trapping agents. It would of course be interesting to explore the mechanistic issue of when this is a rate-determining step, but that is beyond our scope.

The present calculations could be improved in various ways. For example, we could improve our description of the reaction path and reaction path curvature using smaller step sizes in the reaction path propagation, we could compute vibrational frequencies at the stationary points with the larger basis set and interpolate corrections,[37,38] we could use multireference methods to treat electron correlation, we could look at the complex involving $P(CH_3)_3$ ligands instead of PH_3, we could study longer alkanes, we could use curvilinear internal coordinates,[28h] we could include the effect of anharmonicity, we could explore whether large-curvature corner cutting[23c,e,27b,53] increases the amount of tunneling, and we could model the effects of solvent. It seems unlikely, however, that any of these improvements would change our predictions about the coupling of the reaction coordinate to reactant and product vibrational modes or our conclusions about the large magnitude of quantum mechanical zero point and tunneling effects on the rate constant for the rearrangement.

5. Concluding Remarks

There has been considerable effort directed to modeling C−H bond activation processes, but two aspects that have not previously received attention are the roles of vibrations and quantum effects in the dynamics. In the present paper, by employing a direct dynamics method, we were able to study such effects for a 15-atom rearrangement process that serves as a prototype for C−H bond activation processes catalyzed by complexes of late transition metals, namely *trans*-$Rh(PH_3)_2Cl(\eta^2\text{-}CH_4) \rightarrow Rh(PH_3)_2ClH(CH_3)$. We find significant variations of the vibrational frequencies along the reaction path and large quantum effects due to both quantization of vibrational energy (especially zero point energy) and tunneling. For example, at 200 K, these effects enhance the rearrangement by factors of 57 and 3.4, respectively, for an overall speedup of a factor of 194. Even at 300 K the quantum speedup is still large, a factor of 20. Due to the intrinsic participation of hydrogenic motion in the reaction path for C−H bond activation reactions, we anticipate that vibrational quantization effects will generally be large for this kind of reaction (in both homogeneous and heterogeneous catalytic systems) and that tunneling will be important whenever there is an appreciable barrier to reaction.

Acknowledgment. J.E.G. acknowledges the Junta de Extremadura (Spain) for a visiting professor scholarship. J.C.C. acknowledges the Spanish Ministerio de Educación y Cultura and the Fulbright Commission for a postdoctoral scholarship. This work was also supported in part by the U.S. Department of Energy, Office of Basic Energy Sciences.

Supporting Information Available: Full sets of vibrational frequencies for stationary points and the 300 K variational transition state (2 pages). See any current masthead page for ordering and Internet access instructions.

JA972209R

(54) (a) Blais, N. C.; Truhlar, D. G.; Garrett, B. C. *J. Phys. Chem.* **1981**, *85*, 1094. (b) Blais, N. C.; Truhlar, D. G.; Garrett, B. C. *J. Chem. Phys.* **1982**, *76*, 2768. (c) Garrett, B. C.; Truhlar, D. G.; Bowman, J. M.; Wagner, A. F.; Robie, D.; Arepalli, S.; Presser, N.; Gordon, R. J. *J. Am. Chem. Soc.* **1986**, *108*, 3515. (d) Wonchoba, S. E.; Hu, W.-P.; Truhlar, D. G. *Phys. Rev. B* **1995**, *51*, 9985.

(55) Margl, P.; Lohrenz, J. C. W.; Ziegler, T.; Blöchl, P. E. *J. Am. Chem. Soc.* **1996**, *118*, 4434.

(56) Truhlar, D. G.; Garrett, B. C. *Faraday Discuss. Chem. Soc.* **1987**, *84*, 465.

(57) (a) Mayne, H. R. In *Dynamics of Molecules and Chemical Reactions*; Wyatt, R. E., Zhang, G. Z. H., Eds.; Dekker: New York, 1996; p 589. (b) Guo, Y.; Thompson, D. L.; Sewell, T. D. *J. Chem. Phys.* **1996**, *104*, 576.

(58) (a) Garrett, B. C.; Truhlar, D. G. *J. Phys. Chem.* **1979**, *83*, 1079. (b) Chesnavich, W. J.; Bass, L.; Su, T.; Bower, M. T. *J. Chem. Phys.* **1981**, *74*, 2228. (c) Miller, W. H. *J. Chem. Phys.* **1982**, *76*, 2412. (d) Miller, W. H. *J. Phys. Chem.* **1983**, *87*, 21. (e) Garrett, B. C.; Truhlar, D. G.; Wagner, A. F.; Dunning, T. H., Jr. *J. Chem. Phys.* **1983**, *78*, 4400. (f) Steckler, R.; Truhlar, D. G.; Garrett, B. C. *J. Chem. Phys.* **1986**, *84*, 6712. (g) Garrett, B. C.; Truhlar, D. G.; Bowman, J. M.; Wagner, A. F. *J. Phys. Chem.* **1986**, *90*, 4305. (h) Davis, M. J.; Gray, S. K. *J. Chem. Phys.* **1986**, *84*, 5389. (i) Davis, M. J. *J. Chem. Phys.* **1987**, *86*, 3978. (j) Song, K.; Chesnavich, W. J. *J. Chem. Phys.* **1990**, *93*, 5251. (k) Chatfield, D. C.; Friedman, R. S.; Lynch, G. C.; Truhlar, D. G.; Schwenke, D. W. *J. Chem. Phys.* **1993**, *98*, 342.

(59) (a) Chatfield, D. C.; Friedman, R. S.; Schwenke, D. W.; Truhlar, D. G. *J. Phys. Chem.* **1992**, *96*, 2414. (b) Chatfield, D. C.; Friedman, R. S.; Mielke, S. L.; Schwenke, D. W.; Lynch, G. C.; Allison, T. C.; Truhlar, D. G. In *Dynamics of Molecules and Chemical Reactions*; Wyatt, R. E., Zhang, J. Z. H., Eds.; Marcel Dekker: New York, 1996; p 323.